Supplementary Information

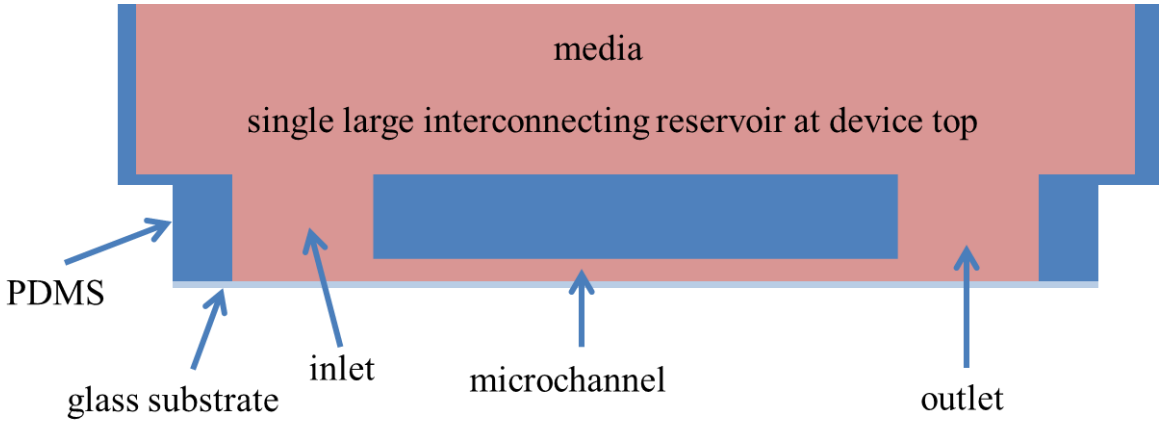

SI Figure 1: Side-view of device. In addition to the features shown in Fig. 1, a single large reservoir with PDMS boundaries is bonded on top of the device, interfacing both the inlet and outlet of the channel. This connects the inlet and outlet to the same media and enables them to be under the same pressure, such that there is no pressure gradient driving flow in the channels. In microfluidic devices, $Q = \Delta P/R$, where Q is the volumetric flow rate in the channels, ΔP is the pressure gradient across the channels, and R is the hydraulic resistance of the channels [1]. In our setup, any applied pressure is gravity driven so $\Delta P = \rho g \Delta h$, where ρ is the fluid density, g is the acceleration due to gravity, and Δh is the liquid height difference between the inlet and outlet of the channel. In our setup at static conditions, because the inlet and outlet are connected to the same unifying reservoir at the top as shown in the figure, $\Delta h = 0$, so Q across the channels due to any externally applied pressures is 0.

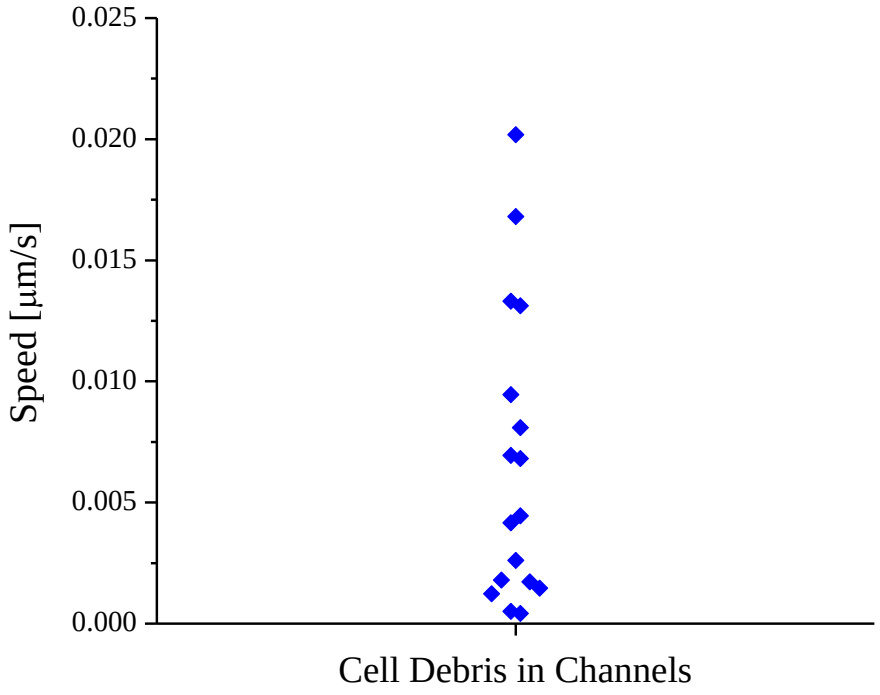

SI Figure 2: To determine if there is substantial flow in the channels, we measured the speeds of actively diffusing cell debris, as shown in SI Video 8. The channel set up is per usual, with a single larger reservoir interfacing both the inlet and outlet at the top such that no pressure gradient is present to actively drive flow. The average particle speed in the channels over a time step of 340 minutes is 0.0067 ± 0.0015 (s.e.m., n=17 particles) µm/s. We used a relatively large time step here to extract potentially small flow rates. Our results show that the particle speeds are much lower than the flow rates used in experiments that demonstrated and mimicked the impact on cell behavior from interstitial flow, which are typically on the order of 1 µm/s [2, 3].

SI Video 1: An MDA-MB-231 cell encounters the decision tree in the circular pattern. It exhibits extensional dynamics that ultimately result in the cell choosing the larger (top) path. Each frame is 10000x real time.

SI Video 2: As the cell encounters the decision tree in the semicircular pattern, split extensions are generated, asymmetric collapse occurs, and finally the cell is polarized along the smaller (bottom) path. Each frame is 10000x real time.

SI Video 3: A Blebbistatin-treated cell navigates through the decision tree. The extensions appear thinner, the cell body is more rounded (likely due to less cell tension), and the cell exhibits a tethered-ball motile state. Each frame is 10000x real time.

SI Video 4: Taxol-treated cells typically are more rounded and have less migratory persistence. Here, a Taxol-treated cell struggles at the decision tree interface. Each frame is 10000x real time.

SI Video 5: An untreated MDA-MB-231 cell enters the ring trap. The subnucleus-scaled entrance focuses the cell and the cell expands symmetrically into the ring region. Eventually, symmetry breaks and the cell undergoes polarized migration. Each frame is 1000x real time.

SI Video 6: Mechanical asymmetries can suppress cell dissemination by confining cell trajectories within the ring region, inducing the phenomenon *iteratio ad nauseam*. Each frame is 10000x real time.

SI Video 7: Cells that divide in the ring trap tend to escape soon thereafter, indicating coupling dynamics between cell proliferation and cell invasion. Each frame is 10000x real time.

SI Video 8: Actively diffusing cell debris are used to track potential flow in the channels. Each frame is 10000x real time. For scale reference, the width of the channel is 15μm.

References

1. H. A. Stone, A. D. Stroock and A. Ajdari, *Annu. Rev. Fluid Mech.*, 2004, **36**, 381-411.
2. W. J. Polacheck, J. L. Charest and R. D. Kamm, *PNAS*, 2011, **108**, 11115-11120.
3. U. Haessler, J. C. M. Teo, D. Foretay, P. Renaud and M. A. Swartz, *Integrative Biology*, 2012, **4**, 401-409.